Available online at www.sciencedirect.com

ScienceDirect

journal homepage: www.elsevier.com/locate/he

Flashback of H_2-enriched premixed flames in perforated burners: Numerical prediction of critical velocity

Filippo Fruzza, Rachele Lamioni, Leonardo Tognotti, Chiara Galletti*

Dipartimento di Ingegneria Civile e Industriale, Università di Pisa, 56122 Pisa, Italy

HIGHLIGHTS

- 2D unsteady simulations of H_2-enriched flames with detailed kinetics to estimate flashback.
- Conjugate Heat Transfer fundamental to predict flashback.
- Flame quenching instead of flashback, for low hydrogen contents.
- Different flashback regimes for different H_2 contents.
- Critical flashback velocity much different from laminar flame speed at high H_2contents.

GRAPHICAL ABSTRACT

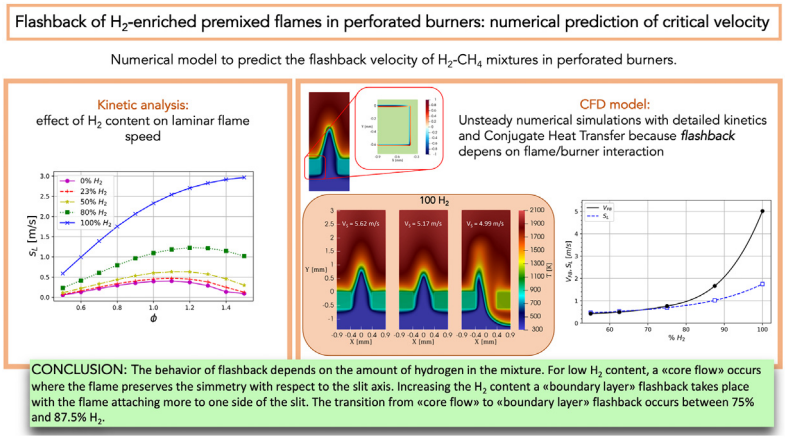

ARTICLE INFO

Article history:
Received 15 February 2023
Received in revised form
19 April 2023
Accepted 22 April 2023
Available online 12 May 2023

Keywords:
Hydrogen
Flashback
Laminar premixed flame
Perforated burner
Decarbonization
Computational fluid dynamics

ABSTRACT

Hydrogen has been identified as a potential tool for decarbonizing various industrial sectors by replacing natural gas while maintaining the combustion-based conversion system. However, due to its high reactivity, hydrogen is prone to flashback, making it essential to implement safety measures for its efficient use in practical appliances. This study investigates the flashback of different H_2/CH_4 mixtures at an equivalence ratio $\varphi = 0.8$ and proposes a numerical model to predict the critical flashback velocity for laminar premixed flames. The model considers the conjugate heat transfer between the gas phase and the burner plate. To overcome the computational cost needed to resolve both gas and burner heating, different time steps are employed for the fluid and the solid domains. Two flashback regimes are identified depending on the H_2 content. The results suggest that using the laminar flame speed alone is inadequate for designing the safe operation of practical premixed burners.

* *Corresponding author.*
E-mail address: rachele.lamioni@unipi.it (R. Lamioni).

https://doi.org/10.1016/j.ijhydene.2023.04.252

Introduction

The recent EU Fit for 55 program highlights the urgent need for a 55% reduction in carbon dioxide (CO_2) emissions by 2030 compared to 1990 levels to ensure a climate-neutral Europe by 2050 [1]. Achieving this goal requires a significant increase in the use of renewable sources of energy to reduce dependence on fossil fuels, as outlined in the REPowerEU action [2]. The residential sector accounts for approximately 30% of final energy consumption, and to meet the aforementioned targets, at least two-thirds of this energy in Europe must be obtained from electricity by 2050. However, the current heating systems primarily rely on gas boilers, making electrification a costly and difficult upgrade [3,4]. To further promote decarbonization, the International Energy Agency has recommended that only zero carbon-ready gas boilers be sold after 2023 [5–7]. This means that these boilers should operate using green hydrogen produced through water electrolysis, using excess wind and solar power. Hydrogen can serve as an energy vector to be burned in gas boilers, utilizing the same technologies and limiting the costs associated with upgrading heating systems [8,9]. Moreover, hydrogen will soon be injected into the existing gas network, up to a 20% concentration, enabling the storage and distribution of renewable energy through existing infrastructure [10–14]. It is anticipated that pipelines able to handle 100% H_2 will be developed, particularly with the creation of regionally integrated hydrogen ecosystems, known as "Hydrogen Valleys", although this will require significant efforts and will occur gradually [15]. It is estimated that hydrogen, either in the form of H_2-admixture from the gas network or as pure H_2 in the hydrogen valleys, could provide up to 18% of the energy needed for domestic heating by 2050 [16].

However, hydrogen exhibits properties that are vastly different from natural gas [17–19]. In particular, the laminar flame speed increases from $S_L = 0.3$ m/s to $S_L = 2.5$ m/s, or approximately six times, when switching from natural gas to hydrogen under stoichiometric conditions. The laminar flame speed, S_L, is defined as the speed at which a flame front propagates relative to the unburnt gas for a freely propagating premixed flame in one dimension. When the flow velocity and the flame front propagation velocity are locally equal on the flame front, the flame is stable. However, if the flow velocity is lower than the flame front propagation velocity, the flame front propagates upstream looking for a new stable configuration. When a stable configuration cannot be found, the flame propagates toward the burner and upstream components, resulting in an undesirable phenomenon called *flashback* [20–22]. Flashback has the potential to cause hazardous situations; hence, devices involving premixed flames must be designed to operate under conditions that prevent the flame from moving upstream into unsuitable zones. This may pose a significant challenge, hindering the application of hydrogen in domestic end-user devices, such as condensing boilers, since modern types of boilers operate in a premixed configuration. Indeed, domestic end-user devices are typically equipped with perforated cylindrical or flat burners which inject a premixed mixture into the combustion chamber and generate short-length flames that fit in the compact volume between the burner and the heat exchanger coils. Recent works, such as the ones by Najarnikoo et al. [23], Lamioni et al. [24,25], and Schiro et al. [26], provide some examples of perforated cylindrical burners. However, the design of burners is mainly based on the manufacturer's experience with conventional fuels, such as natural gas [26]. Thus, it is crucial to carefully analyze the impact of adding H_2 to domestic devices to develop designs that can prevent any flashback phenomena, which could cause serious safety issues [27].

The assessment of flashback velocity in real-world devices can be challenging due to the complex nature of the phenomenon. While laminar flame speed can provide a rough estimate of flashback velocity, other factors such as the physical properties of the fuel (e.g., hydrogen content, reactivity, Lewis number) and flame-wall interaction can significantly influence flashback onset. The laminar flame speed, which is typically measured for freely propagating flames, may not be a reliable indicator of actual flashback velocity in real devices, as demonstrated by experimental studies conducted by de Vries et al. [28] and Aniello et al. [29]. Research on flame stabilization and flashback/blow-off limits of premixed flames dates back to the early 1940s when Lewis and Von Elbe proposed the first flame stabilization theory [30]. However, their "Critical velocity gradient" theory for boundary flashback is only valid for flame holders with negligible thickness [31], and a comprehensive understanding of the phenomenon for real-world applications is still lacking. Factors such as flame curvature, preferential diffusion effects, stretch rate, and conjugate heat transfer between the flame and the burner are critical for flame stabilization [32–42]. In particular, flame-wall interactions play a key role in the flashback dynamics. Kurdyumov et al. [43] showed the importance of wall heat losses by comparing adiabatic and cold wall conditions. Kiymaz et al. [44] studied the wall temperature effects on the flashback propensity in Bunsen-type burners. Both these works highlighted the importance of the conjugate heat transfer (CHT) between the flame and the solid burner. Vance et al. [45] studied the flashback limits of premixed hydrogen flames in multi-slit burners, modeling both fluid and solid zones and including CHT in their investigation. Recently, Pers et al. [46] evaluated experimentally the impact of wall temperature on flashback for H_2-enriched methane-air flames, by investigating the possibility of autoignition as a flashback initiation mechanism.

This study aims to numerically investigate the flashback phenomenon in perforated burners by assessing the flashback velocities of various H_2/CH_4 mixtures to quantify their propensity to flashback. The investigation employs 2-D transient numerical simulations with detailed kinetics to characterize the flame coming from a slit commonly found in perforated burners. Due to the small dimensions of the slit and the low velocities, the problem is completely laminar, and no turbulence model is needed. Symmetric boundary conditions are employed to mimic the actual pattern of the slits. As the interaction between the burner plate and the mixture is crucial in flame stabilization, the numerical model encompasses the corresponding solid domain and the conjugate heat transfer between the flame and the burner. To account for the significant differences between the chemistry and heat conduction time scales, a solid time step is introduced. Additionally, the model considers radiation and thermo-diffusive effects. The predicted flashback velocity is compared with the

laminar flame speed, which is estimated through 1-D simulations of freely propagating flames.

Numerical model

In this study, we investigate a multi-slit configuration representing a portion of a real burner commonly used in domestic condensing boilers. Preliminary 1-D free-propagating flames are simulated using the Cantera [47] kinetic open-source processor, to analyze the flame characteristics for different H_2 content from 0% to 100% by vol. and equivalent ratio φ from 0.5 to 1.5, where the equivalence ratio is defined as $\varphi = \frac{n_f/n_{ox}}{(n_f/n_{ox})_{st}}$ with n_f and n_{ox} representing the molar flow rate of the fuel and oxidizer, respectively. The st subscript denotes the stoichiometric conditions. Subsequently, a 2-D model is developed with computational fluid dynamics (CFD) techniques in unsteady conditions to capture the flashback phenomenon for different contents of H_2 in the range 55–100% by vol. at $\varphi = 0.8$. Indeed, as will be discussed in Section 3.4, no flashback was observed with lower hydrogen contents for the given geometrical configuration.

Computational domain and grid

The computational domain is represented by a 2-D slit, as shown in Fig. 1, where the burner is depicted in black. To avoid the influence of boundary conditions and to enclose the flame even in flashback conditions, the domain extends 10 mm downstream and 6 mm upstream of the solid. The width of the slit is $W = 0.8$ mm, and the distance between two adjacent slits is 1 mm, resulting in a total domain width of $D = 1.8$ mm. The thickness of the burner is 0.6 mm. The structured computational grid was generated using g-mesh [48]. The size of the grid cells in the reaction front region was chosen to be 25 μm based on preliminary 1-D simulations of freely propagating flames conducted using the open-source code Cantera [47]. Specifically, the cell size was chosen such that at least 15 nodes were contained within the thermal flame thickness l_T, which was calculated using the temperature profiles as [49].

$$l_T = \frac{T_b - T_u}{|dT/dx|_{max}}, \tag{1}$$

where T_b and T_u are the temperatures of the burnt and fresh gases, respectively, and dT/dx is the temperature gradient. A grid independence study was performed under both steady and transient conditions with 100% H_2, as this mixture requires higher mesh resolution due to the lower thermal flame thickness.

Physical model

The problem may be described by conservation equations for mass, momentum, and energy, and the transport/reaction equations for the chemical species in the gas phase under steady and unsteady conditions. As the problem is entirely laminar, and the maximum jet Reynolds number across all investigated cases is approximately $Re = 120$, a turbulence model is not utilized. The system of governing equations is

$$\frac{\partial \rho}{\partial t} + \nabla\cdot(\rho \mathbf{v}) = 0 \tag{2}$$

$$\frac{\partial}{\partial t}(\rho \mathbf{v}) + \nabla\cdot(\rho \mathbf{v}\mathbf{v}) = -\nabla p + \nabla\cdot(\bar{\bar{\tau}}) \tag{3}$$

$$\frac{\partial}{\partial t}(\rho E) + \nabla\cdot(\mathbf{v}(\rho E + p)) = \nabla\cdot\left(k\nabla T + \sum_j h_j\left(\rho D_{m,j}\nabla Y_j + D_{T,j}\frac{\nabla T}{T}\right)\right) - \sum_j h_j\omega_j + S_{rad} \tag{4}$$

$$\frac{\partial}{\partial t}(\rho Y_i) + \nabla\cdot(\rho \mathbf{v} Y_i) = \nabla\cdot\left(\rho D_{m,i}\nabla Y_i + D_{T,i}\frac{\nabla T}{T}\right) + \omega_i, \tag{5}$$

where ρ is the density, $\mathbf{v}$ is the velocity vector, p is the pressure and $\bar{\bar{\tau}}$ is the stress tensor. The ideal gas equation of state is used for the density. h_j, Y_j and ω_j are the enthalpy, the mass fraction, and the net rate of production of the jth species respectively, and $E = \sum_j h_j Y_j - p/\rho + v^2/2$. k is the mass-weighted thermal conductivity of the mixture, $D_{m,j}$ and $D_{T,j}$ are the generalized mass and thermal diffusion coefficients of the jth species [50–52]. Finally, S_{rad} is the energy source associated with radiation. In both 1-D and CFD models, we employed the Kee-58 mechanism with 17 chemical species and 58 reversible reactions [53]. The latter model, although skeletal, has been widely used for H2NG blends (50%H_2/50% CH_4 by vol.) [54]. Besides we bench-marked this model against the complete GRI3.0 model in Refs. [24,55] for the simulation of a multi-hole burner of domestic boilers. Full multicomponent diffusion is modeled through the definition of generalized Fick's law coefficients derived by the Maxwell-Stefan equations [50–52]. Soret diffusion is modeled using an empirically-based formula provided by Kuo [56]. Radiation is modeled through the Discrete Ordinates (DO) method [57], with

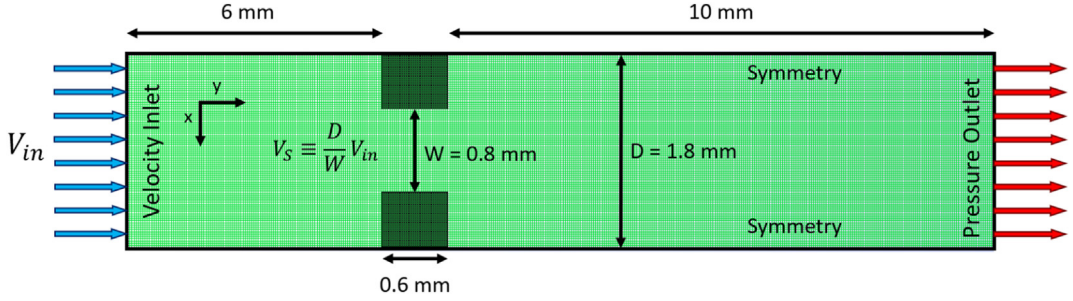

Fig. 1 – Computational domain.

weighted-sum-of-gray-gases model, assuming the emissivity of radiation of the fluid-solid interface to be 0.85. The burner emissivity has been analyzed to determine its effect on burner temperatures and flashback velocity. Various sources in the literature [45,58–60] place the emissivity range of steel burners between 0.75 and 0.95. Our analysis, reported in the Supplementary Material, showed that only minor differences are observed within this range.

The conjugate heat transfer between the fluid and the solid zones is modeled to take into account the interaction between the flame and the burner plate, as this mechanism plays a major role in flame stabilization and, we expect, in triggering flashback. The CHT is modeled by using Fourier's Law to compute the heat flux through the fluid-solid interface [50].

$$q = k\frac{\partial T}{\partial \mathbf{n}}\bigg|_{\text{wall}} + q_{\text{rad}} \tag{6}$$

where q is the heat flux, k is the thermal conductivity of the fluid, $\mathbf{n}$ is the local coordinate normal to the wall and q_{rad} is the heat flux due to radiation, responsible of the radiative heat losses of the burner to the surroundings. In the solid domain, representing the burner plate, we resolve the energy equation, i.e.

$$\frac{\partial}{\partial t}(\rho_s h_s) = \nabla\cdot(k_s \nabla T) \tag{7}$$

where ρ_s, k_s and $h_s = \int_{T_0}^{T} c_{p,s} dT$ are the density, the thermal conductivity, and the sensible enthalpy of the solid material. Here, the properties of the stainless steel typically used for this kind of burner are employed, i.e density $\rho_s = 7719\ \text{kg m}^{-3}$, specific heat $c_{p,s} = 461.3\ \text{J kg}^{-1}\ \text{K}^{-1}$, and thermal conductivity $k_s = 22.54\ \text{W m}^{-1}\ \text{K}^{-1}$. The inclusion of CHT is necessary since there is no straightforward method to predict the burner temperature for a particular mixture at a specific inlet velocity. The burner temperature has a significant influence on the flashback dynamics due to the substantial impact of the fluid velocity on its density, and the fresh mixture preheating on the flame speed. A comprehensive investigation of these effects, as well as a comparison of CHT with other modeling techniques such as isothermal and adiabatic walls, is presented in Effect of flame-wall interaction.

Boundary conditions

Uniform velocity and uniform temperature of $T_u = 300$ K are set at the inlet, while a pressure outlet with $p = 1$ atm is imposed at the exit of the domain. The external edges of the domain are modeled as symmetry boundaries to account for the interaction with flames from nearby slits. Specifically, zero normal velocity and zero normal gradients of all variables are imposed at the symmetry plane. At the fluid-solid interface, a no-slip boundary condition is given for velocity, while no thermal boundary conditions are needed since heat fluxes are computed directly using the CHT model.

Solution methodology

Initially, steady-state simulations are performed to obtain a stable and developed flame configuration for different H_2 contents, specifically 55%, 62.5%, 75%, 87.5%, and 100% by vol., at a fixed equivalence ratio of $\varphi = 0.8$. The governing equations are solved using the pressure-based coupled algorithm available in ANSYS-FLUENT 22.1 [50], with a second-order upwind scheme. The inlet velocity $\widetilde{V}_{in}$ utilized in the steady simulations for each mixture is provided in Table 1. To investigate flashback, transient simulations are performed using a second-order implicit method with the PISO solver. Starting from the stable flame obtained in steady-state conditions reported in the Supplementary Material, the inlet velocity is gradually reduced until flashback occurs. The inlet velocity is reduced in steps of $\Delta V_{in} = 0.1$ m/s, with an additional refinement of $\Delta V_{in} = 0.01$ m/s when approaching the flashback limit. After reducing the inlet velocity, the flame and the burner temperature are allowed to stabilize before reducing the velocity again. Once the critical velocity is reached, flashback is observed. This method allows for the estimation of the flashback velocity for each mixture. We point out that no thermodiffusive instabilities are observed in all simulations. We define the *cold-flow* bulk velocity at the slit entry as

$$V_S = \frac{A_{tot}}{A_{slit}} V_{in}, \tag{8}$$

where V_{in} is the uniform inlet velocity. V_S is the velocity we would have for a cold flow, i.e., neglecting the density variations of the mixture due to the high burner plate temperatures. We define the flashback velocity V_{FB} as V_S when flashback occurs

$$V_{FB} = V_S|_{FB} = \frac{A_{tot}}{A_{slit}} V_{in}|_{FB}. \tag{9}$$

The time steps employed for each mixture are determined based on their characteristic chemical timescale, and their values are presented in Table 1. Since the characteristic timescales for the reactive flow in the fluid domain and the heat conduction within the solid domain are significantly different, with the burner temperature stabilization time typically in the order of seconds, a uniform time step across the entire computational domain cannot be used for computational efficiency reasons. To expedite heat conduction within the solid while maintaining the accuracy of the flow solution, a different time step is used for the solid zone, with $\Delta t_s \approx 10^3 - 10^4 \Delta t$. The solid time step values used for each mixture can be found in Table 1. The uniqueness of the solution in stable regimes and consistency of flashback velocities are verified using different solid time steps of 0.01 ms, 0.1 ms, and 1 ms for the 100% H_2 case. No variations are observed in the burner plate temperatures of stable configurations or the estimated flashback velocity.

Table 1 – Parameters of steady and transient simulations for the different H_2/CH_4 mixtures.

H_2 [% by vol.]	CH_4 [% by vol.]	$\widetilde{V}_{in}$ [m/s]	Δt [μs]	Δt_s [ms]
55	45	0.8	5	1
62.5	37.5	1.0	4	1
75	25	1.4	3	1
87.5	12.5	2.0	2	1
100	0	3.2	1	1

Results

1-D preliminary analysis

We conduct a preliminary analysis using Cantera [47] to examine 1-D freely-propagating premixed flames and assess their characteristics under different operating conditions in terms of equivalence ratio (ranging from 0.5 to 1.5) and H_2 content (varying from 0% to 100% by volume). We perform simulations under the same mixture conditions ($T = 300$ K, $p = 1$ atm) as those used in 2-D. Fig. 2 illustrates the laminar flame speed S_L, adiabatic flame temperature T_a, and thermal flame thickness l_T, calculated as $l_T = \frac{T_b - T_u}{|dT/dx|_{max}}$ [49], as a function of the equivalence ratio φ for different H_2 contents. It can be seen that as the H_2 content in the mixture increases, the adiabatic flame temperature rises, while the flame thickness declines. Moreover, the laminar flame speed substantially increases, indicating a higher propensity for the flashback.

2-D transient simulations

Initially, steady-state simulations on the 2-D slit domain are performed for each H_2 content, i.e., 55, 62.5, 75, 87.5, and 100% by vol. at fixed equivalence ratio $\varphi = 0.8$. Then, transient simulations are carried out using the steady-state solutions as initial conditions. The procedure details are available in Solution methodology. Fig. 3 displays the temperature field for three simulation snapshots taken at different inlet velocities, or equivalently, different V_S, for 55% H_2 content. The first two snapshots depict the stable flame configurations obtained at the corresponding velocities. The third snapshot is taken as the flashback occurrence (and hence does not represent an equilibrium solution), and the corresponding velocity V_S is considered the flashback velocity V_{FB}. For this mixture, we observe a "core flow" flashback: the flashback occurs smoothly, with the flame front moving toward the slit entry, flattening, heating up the burner, and then passing through the slit symmetrically. The same dynamics can be observed for 62.5% and 75% H_2, whose temperature fields are reported in a similar way in Figs. 4 and 5 respectively. It is worth noting that increasing the H_2 content leads to a higher velocity onset of flashback, with $V_{FB} = 0.40$ m/s at 55% H_2, $V_{FB} = 0.47$ m/s at 62.5% H_2, and $V_{FB} = 0.74$ m/s at 75% H_2.

The flashback dynamics undergo significant changes when transitioning to higher H_2 concentrations. Figs. 6 and 7 present the temperature field at three different time steps and three distinct inlet velocities for 87.5% and 100% H_2, respectively. The typical dynamics of a "boundary layer" flashback can be observed, with the flashback being initiated suddenly and asymmetrically at the burner wall. Additionally, the flashback velocities increase even more rapidly, with $V_{FB} = 1.64$ m/s at

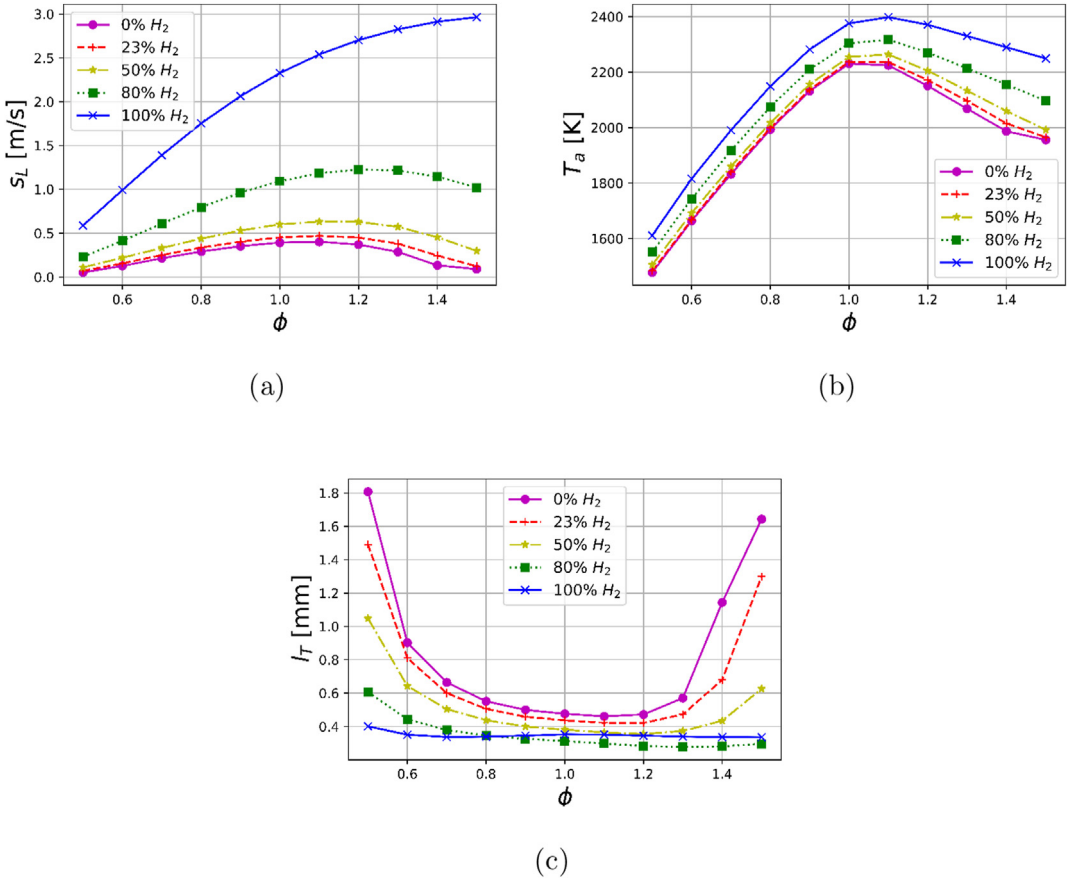

Fig. 2 – Laminar velocity S_L (a), adiabatic temperature (b) and thermal flame thickness l_T (c) for different equivalence ratios φ and H_2 volume fractions in the mixture, computed for 1-D planar flames with Cantera.

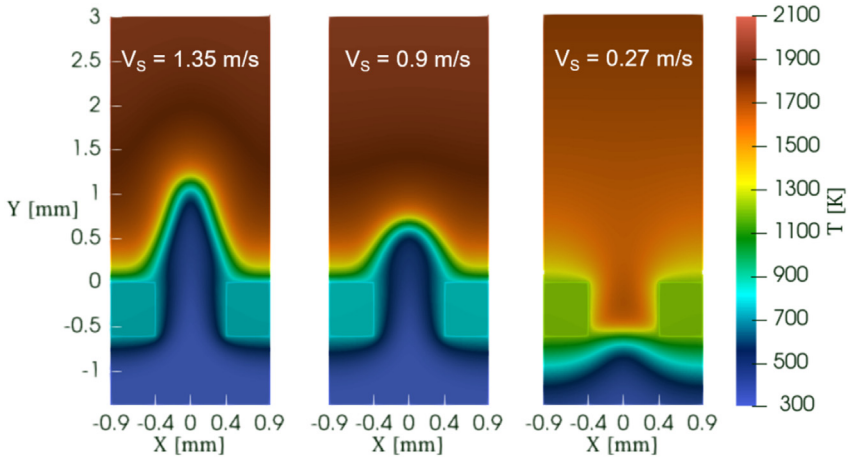

Fig. 3 – Temperature field for decreasing inlet velocity - 55% H_2 and $\phi = 0.8$.

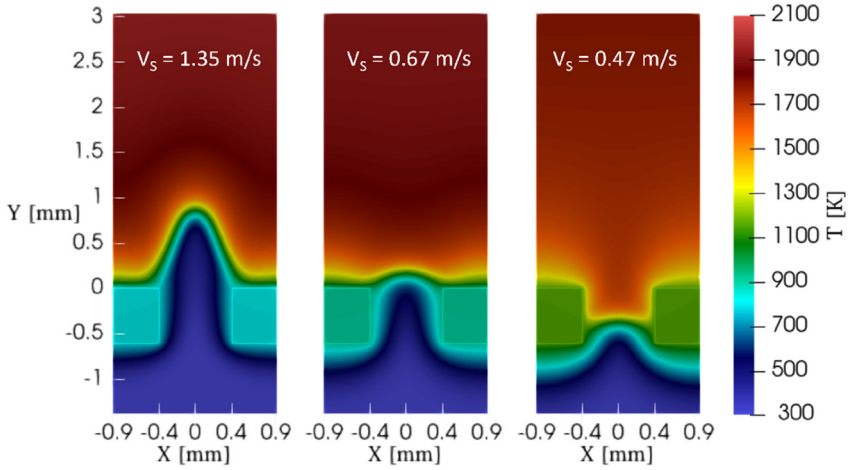

Fig. 4 – Temperature field for decreasing inlet velocity - 62.5% H_2 and $\phi = 0.8$.

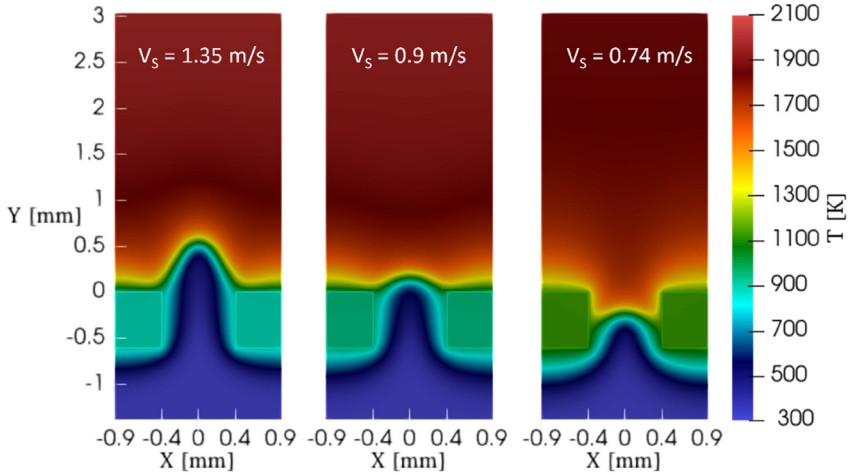

Fig. 5 – Temperature field for decreasing inlet velocity - 75% H_2 and $\phi = 0.8$.

87.5% H_2 and $V_{FB} = 4.99$ m/s at 100% H_2. This transition from a "core flow flashback" regime to a "boundary layer flashback" regime may be due to the higher reactivity of the mixtures, which could promote the ignition of fresh gases at the hot wall. Another factor could be the effect of the low effective Lewis number of hydrogen-rich mixtures, which could disfavor the flame stability in the positive curvature region at the flame base, near the wall. It is worth mentioning that the

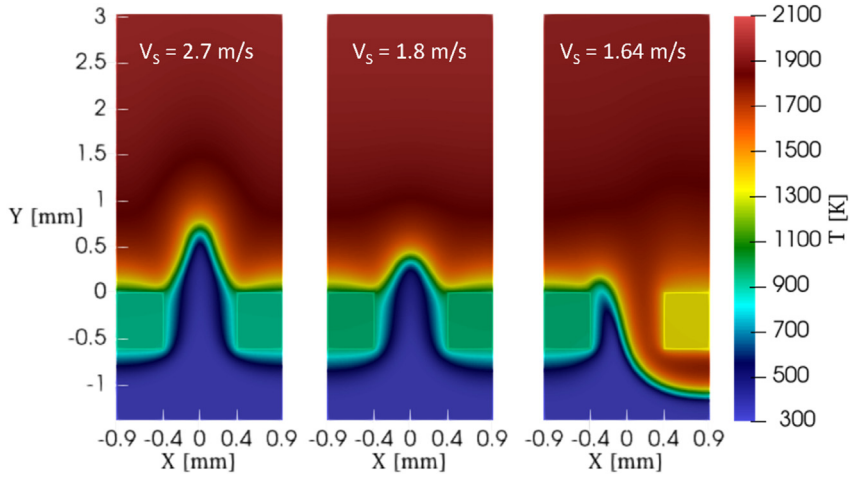

Fig. 6 – Temperature field for decreasing inlet velocity - 87.5% H_2 and $\phi = 0.8$.

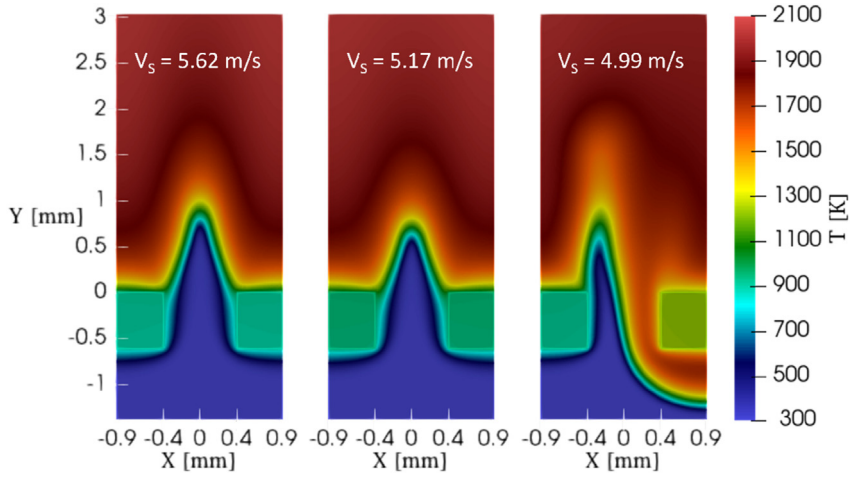

Fig. 7 – Temperature field for decreasing inlet velocity - 100% H_2 and $\phi = 0.8$.

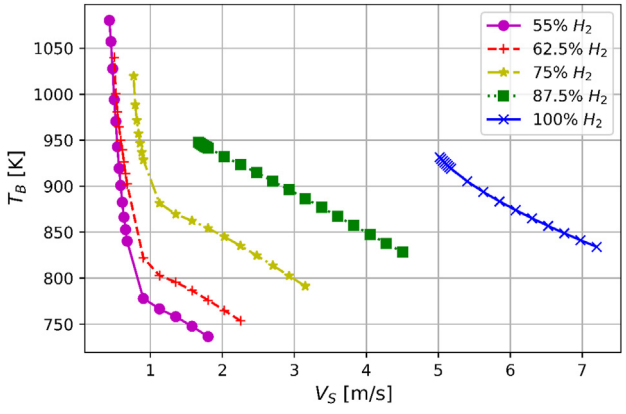

Fig. 8 – Average burner temperature as a function of V_S for different H_2 content at $\phi = 0.8$.

flashback velocity for 100% H_2 is consistent with the results obtained in a similar configuration by Vance et al. in their recent work [45].

Fig. 8 depicts the average burner temperature as a function of the velocity at the slit entry V_S for the five different mixtures investigated in this study. The last point on the left of each curve represents the flashback limit of the corresponding case. It can be observed that the burner temperature generally decreases with decreasing hydrogen content under stable operating conditions (high velocity). For mixtures containing 87.5% and 100% H_2, which fall under the "boundary layer" flashback regime, the burner temperature exhibits a quasi-linear relationship with the inlet velocity until the flashback limit is reached. In contrast, mixtures containing 55% H_2, 62.5% H_2, and 75% H_2, which fall under the "core flow" flashback regime, exhibit a significant deviation from the linear trend, with the burner temperature increasing steeply as the flashback limit is approached. This effect can be attributed to the fact that the "core flow" flashback regime allows for stable flame configurations that are located in close proximity to the slit exit, leading to the overheating of the burner. It should be noted that our model is not capable of predicting flashback resulting from the autoignition of the combustible mixture near the hot wall inside the burner, which typically occurs for

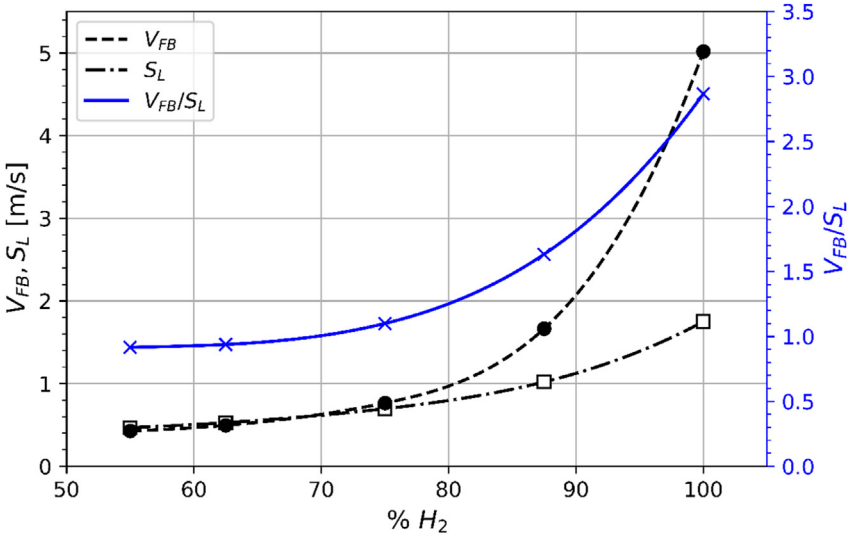

Fig. 9 – Flashback velocity, laminar flame speed, and their ratio as a function of H_2 content at $\phi = 0.8$.

the same range of hydrogen content and burner temperatures found in the "core flow" regime [46].

To illustrate the propensity for flashback in each mixture, we normalize the flashback velocities with the corresponding laminar flame speeds, which were obtained from 1-D simulations performed using CANTERA under standard conditions ($T = 300$ K, $p = 1$ atm). Fig. 9 displays the estimated flashback velocity V_{FB}, the laminar flame speed S_L, and their ratio V_{FB}/S_L as functions of the hydrogen content in the fuel. As expected, V_{FB} increases significantly with increasing hydrogen content. The laminar flame speed also increases with the hydrogen content, but this increase is more uniform across the entire composition range. Consequently, the V_{FB}/S_L ratio increases monotonically with the hydrogen content, exhibiting a very strong dependence at high H_2 contents. Notably, the slope of the V_{FB} curve shows a sharp increase in steepness when transitioning from the "core flow" flashback regime to the "boundary layer" flashback regime. We note that the model tends to overestimate the heating rate of the burner plate during flashback, i.e., when the flame front moves back and crosses the slit, due to the difference in time steps between the solid and fluid zones. Specifically, the burner temperature rapidly increases from approximately 900 K to around 1300 K within a time span in the fluid zone of 1 ms following the onset of flashback. This observation suggests that the heating rate is overestimated as the flame front crosses the slit. However, this is the normal consequence of the much larger solid time step that is set to avoid an unfeasible computational cost. Nonetheless, the model is capable of capturing the onset of the flashback phenomenon, which is sufficient for estimating the flashback velocity.

Effect of flame-wall interaction

In this section, we compare the results obtained by modeling the conjugate heat transfer between the fluid and the solid phases and two different modeling approaches commonly found in the literature for flashback analysis, i.e., isothermal and adiabatic walls [43,44]. To this end, we apply the procedure described above to compute the flashback velocity of the 100% H_2 and $\varphi = 0.8$ mixture for the same geometry but solving only the gas phase and imposing four different isothermal boundary conditions (T_{wall} = 700 K, 800 K, 900 K, 1000 K) and an adiabatic (zero heat flux) boundary condition at the fluid-solid interface. Fig. 10 shows the flashback velocity estimated as a function of wall temperature for isothermal walls (black solid line) and two horizontal lines representing the flashback velocities computed with adiabatic walls (blue dashed line) and CHT (red dashed-dotted line). The plot indicates that the flashback velocity V_{FB} is highly dependent on the isothermal wall temperature. Specifically, V_{FB} is almost five times larger for $T_{wall} = 1000$ K compared to $T_{wall} = 700$ K. However, since the burner temperature at the flashback limit is not known and depends on the hydrogen content, as pointed out in Fig. 8, a fixed wall temperature cannot be used to estimate the flashback velocity accurately. Moreover, the result obtained with the CHT approach is approximately twice the value obtained with adiabatic walls, indicating that the latter approach is also not suitable for accurate calculations.

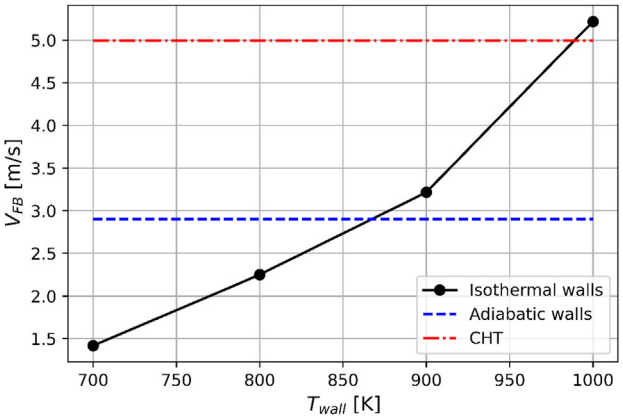

Fig. 10 – Flashback velocity for 100% H_2 and $\phi = 0.8$ with different flame-wall interaction models: isothermal walls, adiabatic walls, and CHT.

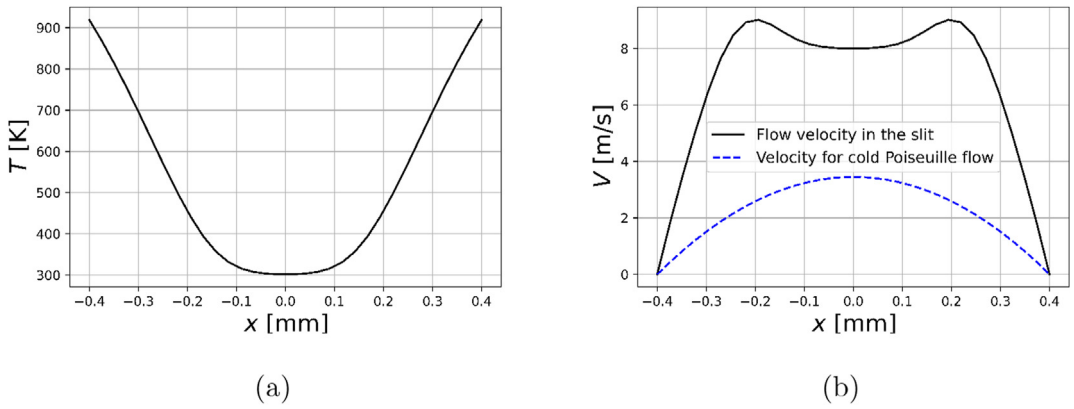

Fig. 11 – Temperature and velocity profiles inside the slit for 100% H_2 and $\phi = 0.8$ at $V_S = 2.3$ m/s.

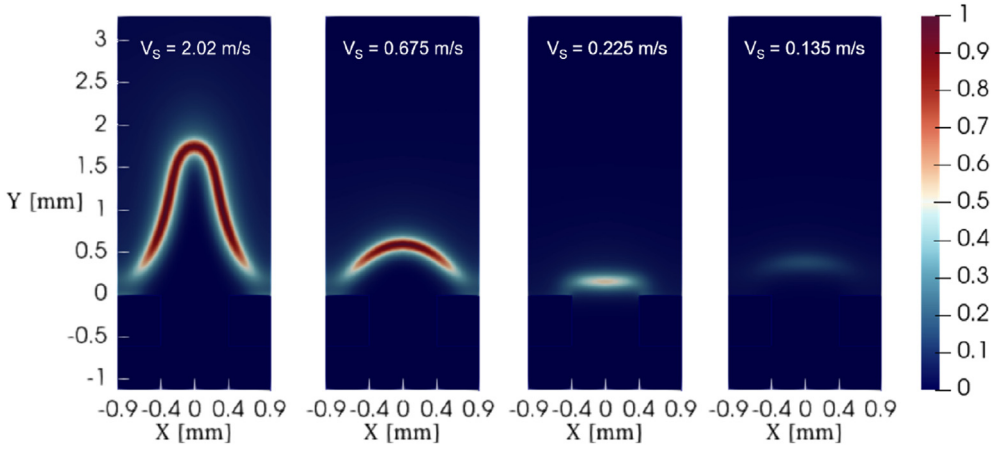

Fig. 12 – Field of heat release rate normalized to the maximum value for decreasing inlet velocity - 40% H_2 and $\phi = 0.8$.

To investigate the impact of unburnt mixture preheating inside the slit resulting from the hot burner walls, temperature and velocity profiles are analyzed. Fig. 11 presents the profiles along a line going from one wall to the other and lying halfway between the exit and the entrance of the slit, for the 100% H_2 and $\varphi = 0.8$ mixture at $V_S = 2.3$ m/s. In addition, the velocity profile for the cold fully developed Poiseuille flow expected in the absence of preheating are plotted as a reference. The results show that mixture preheating plays a significant role in increasing the flow velocity by reducing the mixture density, thereby reducing the risk of flashback. On the other hand, the mixture preheating has an important effect on increasing the flame speed, thus favoring flashback. The complex interplay between these opposing effects is critical to understanding flashback dynamics. Therefore, we believe that an accurate model for flame-wall interaction using the CHT approach is essential to estimate flashback velocities in multi-slit burners.

Flame quenching for low hydrogen contents

The hydrogen percentage range investigated in this study, specifically 55–100% by volume, is selected because we do not observe any flashback for hydrogen contents below 55% at a stoichiometric ratio of 0.8 for our configuration. For lower hydrogen contents, our model predicts that the flame will extinguish as the inlet velocity is reduced. This phenomenon is illustrated in Fig. 12, which shows the normalized heat release rate of the 40% H_2 mixture at four different inlet velocities during the transient simulation. As the flow velocity decreases, the flame front moves closer to the slit until the heat losses to the burner surpass the heat production from the reaction, leading to flame extinction as indicated by the sharp drop in the heat release rate.

Conclusions

In this study, we present a numerical model for estimating the velocity at which flashback occurs. The model incorporates both fluid and solid domains using the conjugate heat transfer approach, as the flashback is initiated by the interaction between the flame and the burner plate. This interaction presents a major challenge since solid heating is characterized by temporal scales that are significantly larger than those of the fluid, leading to a high computational cost. To overcome this challenge, we used different time steps for the fluid and solid zones. The model is applied to a 2-D geometry that simulates an array of slits, commonly found in practical perforated burners.

Our results indicate that the behavior of flashback differs based on the hydrogen content, when keeping the equivalence ratio fixed at $\varphi = 0.8$. For low amounts of hydrogen, a "core flow" flashback is observed, where the flame gradually moves back through the slit, preserving its symmetry with respect to the slit axis. However, increasing the hydrogen content results in a loss of symmetry, and a "boundary layer" flashback is observed, where the flame attaches more to one side of the slit than the other while returning back to the entrance. This transition from "core flow" to "boundary layer" flashback occurs between 75% H_2 and 87.5% H_2. To further clarify our model, we compared the conjugate heat transfer approach to numerical models for flashback calculation based solely on the treatment of the gas phase and pre-assigned boundary conditions, such as fixed temperature or adiabatic condition. We observe that the use of a fixed temperature at the burner plate leads to a critical flashback velocity that is highly dependent on the chosen temperature values. Conversely, the adiabatic condition leads to very different results from the conjugate heat transfer, such as a critical flashback velocity that is much lower (about 50%). Furthermore, our results highlight that the laminar flame speed can only provide a limited indication of the flashback velocity. This is due to the strong dependence of the flashback velocity on the flame-wall interaction, which is not considered in the conventional estimates of flashback velocity using the laminar speed obtained from 1-D freely propagating flames. We demonstrate that the ratio between the flashback velocity and the laminar flame speed increases with the hydrogen content. Specifically, for 100% H_2, flashback occurs at a velocity that is nearly three times the laminar flame speed, indicating that a simplistic estimation based on S_L cannot be relied upon to determine the conditions for safe operation.

We believe that our model, with its reasonable computational cost, can assist in the design of burners for the efficient and safe use of hydrogen. In the future, it would be of interest to apply the same model under different operating conditions and geometrical configurations, such as varying φ and the slit width W, as we expect this could affect the flashback velocities. Although our model is 2-D, it can be readily applied to 3-D problems with manageable computational efforts. This approach may enable virtual prototyping to be used to find solutions that reduce the flashback tendency of novel fuels.

Author contributions

Filippo Fruzza and Rachele Lamioni: Conceptualization, Methodology, Data curation, Writing-Original draft preparation. Leonardo Tognotti: Reviewing and Editing. Chiara Galletti: Conceptualization, Methodology, Writing-Original draft preparation.

Declaration of Competing Interest

The authors declare that they have no known competing financial interests or personal relationships that could have appeared to influence the work reported in this paper.

Acknowledgements

This research is supported by the Italian Ministry of University and Research (MUR) as part of the PON 2014–2020 "Research and Innovation" resources - Green/Innovation Action - DM MUR 1061/2021 and DM MUR 1062/2021. The authors thank Immergas S.p.A., Brescello, RE (Italy) for partially funding the Ph.D. scholarship.

Appendix A. Supplementary data

Supplementary data to this article can be found online at https://doi.org/10.1016/j.ijhydene.2023.04.252.

REFERENCES

[1] EU Commission Press Release European Green Deal: The Commission proposes transformation of EU economy and society to meet climate ambitions.
[2] REPowerEU: A plan to rapidly reduce dependence on Russian fossil fuels and fast forward the green transition.
[3] Gahleitner G. Hydrogen from renewable electricity: an international review of power-to-gas pilot plants for stationary applications. Int J Hydrogen Energy 2013;38(5):2039–61. https://doi.org/10.1016/j.ijhydene.2012.12.010.
[4] Quarton CJ, Samsatli S. Should we inject hydrogen into gas grids? practicalities and whole-system value chain optimisation. Appl Energy 2020;275:115172. https://doi.org/10.1016/j.apenergy.2020.115172.
[5] Mouli-Castillo J, Orr G, Thomas J, Hardy N, Crowther M, Haszeldine RS, Wheeldon M, McIntosh A. A comparative study of odorants for gas escape detection of natural gas and hydrogen. Int J Hydrogen Energy 2021;46(27):14881–93. https://doi.org/10.1016/j.ijhydene.2021.01.211.
[6] Dawood F, Anda M, Shafiullah G. Hydrogen production for energy: an overview. Int J Hydrogen Energy 2020;45(7):3847–69. https://doi.org/10.1016/j.ijhydene.2019.12.059.
[7] Yang H, Lin X, Pan H, Greg S, Chen Z, Liu Y. Energy saving analysis and thermal performance evaluation of a hydrogen-enriched natural gas-fired condensing boiler. Int J Hydrogen Energy 2023. https://doi.org/10.1016/j.ijhydene.2023.02.027.
[8] McKenna R, Bchini Q, Weinand J, Michaelis J, König S, Köppel W, Fichtner W. The future role of power-to-gas in the energy transition: regional and local techno-economic analyses in baden-württemberg. Appl Energy 2018;212:386–400. https://doi.org/10.1016/j.apenergy.2017.12.017.
[9] Michalski J, Bünger U, Crotogino F, Donadei S, Schneider G-S, Pregger T, Cao K-K, Heide D. Hydrogen generation by electrolysis and storage in salt caverns: potentials, economics and systems aspects with regard to the German energy transition. Int J Hydrogen Energy 2017;42(19):13427–43. https://doi.org/10.1016/j.ijhydene.2017.02.102.
[10] Smith C, Mouli-Castillo J, van der Horst D, Haszeldine S, Lane M. Towards a 100% hydrogen domestic gas network: regulatory and commercial barriers to the first demonstrator project in the United Kingdom. Int J Hydrogen Energy 2022;47(55):23071–83. https://doi.org/10.1016/j.ijhydene.2022.05.123.

[11] Zhao Y, McDonell V, Samuelsen S. Experimental assessment of the combustion performance of an oven burner operated on pipeline natural gas mixed with hydrogen. Int J Hydrogen Energy 2019;44(47):26049–62. https://doi.org/10.1016/j.ijhydene.2019.08.011.
[12] Zhao Y, McDonell V, Samuelsen S. Influence of hydrogen addition to pipeline natural gas on the combustion performance of a cooktop burner. Int J Hydrogen Energy 2019;44(23):12239–53. https://doi.org/10.1016/j.ijhydene.2019.03.100.
[13] de Vries H, Levinsky HB. Flashback, burning velocities and hydrogen admixture: domestic appliance approval, gas regulation and appliance development. Appl Energy 2020;259:114116. https://doi.org/10.1016/j.apenergy.2019.114116.
[14] Wu X, Zhang H, Yang M, Jia W, Qiu Y, Lan L. From the perspective of new technology of blending hydrogen into natural gas pipelines transmission: mechanism, experimental study, and suggestions for further work of hydrogen embrittlement in high-strength pipeline steels. Int J Hydrogen Energy 2022;47(12):8071–90. https://doi.org/10.1016/j.ijhydene.2021.12.108.
[15] Kovač A, Paranos M, Marciuš D. Hydrogen in energy transition: a review. Int J Hydrogen Energy 2021;46(16):10016–35. https://doi.org/10.1016/j.ijhydene.2020.11.256.
[16] Fuel Cells and Hydrogen 2 Joint Undertaking, Hydrogen roadmap Europe : a sustainable pathway for the European energy transition. Publications Office; 2019. https://data.europa.eu/doi/10.2843/341510.
[17] Halter F, Chauveau C, Gökalp I. Characterization of the effects of hydrogen addition in premixed methane/air flames. Int J Hydrogen Energy 2007;32(13):2585–92, iCHS-2005. https://doi.org/10.1016/j.ijhydene.2006.11.033.
[18] Pan H, Geng S, Yang H, Zhang G, Bian H, Liu Y. Influence of H_2 blending on NOx production in natural gas combustion: mechanism comparison and reaction routes. Int J Hydrogen Energy 2023;48(2):784–97. https://doi.org/10.1016/j.ijhydene.2022.09.251.
[19] Liu Y, Zhang Y, Liu X, Liu Z, Che D. Experimental and numerical investigation on premixed H_2/air combustion. Int J Hydrogen Energy 2016;41(24):10496–506. https://doi.org/10.1016/j.ijhydene.2016.01.049.
[20] Kurdyumov V, Fernández E, Liñán A. Flame flashback and propagation of premixed flames near a wall. Proc Combust Inst 2000;28(2):1883–9. https://doi.org/10.1016/S0082-0784(00)80592-5.
[21] Su S-S, Hwang S-J, Lai W-H. On a porous medium combustor for hydrogen flame stabilization and operation. Int J Hydrogen Energy 2014;39(36):21307–16. https://doi.org/10.1016/j.ijhydene.2014.10.059.
[22] Jiménez C, Fernández-Galisteo D, Kurdyumov VN. Dns study of the propagation and flashback conditions of lean hydrogen-air flames in narrow channels: symmetric and non-symmetric solutions. Int J Hydrogen Energy 2015;40(36):12541–9. https://doi.org/10.1016/j.ijhydene.2015.07.037.
[23] Najarnikoo M, Targhi MZ, Pasdarshahri H. Experimental study on the flame stability and color characterization of cylindrical premixed perforated burner of condensing boiler by image processing method. Energy 2019;189:116130. https://doi.org/10.1016/j.energy.2019.116130.
[24] Lamioni R, Bronzoni C, Folli M, Tognotti L, Galletti C. Feeding H_2-admixtures to domestic condensing boilers: numerical simulations of combustion and pollutant formation in multi-hole burners. Appl Energy 2022;309:118379. https://doi.org/10.1016/j.apenergy.2021.118379.
[25] Lamioni R, Bronzoni C, Folli M, Tognotti L, Galletti C. Impact of H_2-enriched natural gas on pollutant emissions from domestic condensing boilers: numerical simulations of the combustion chamber. Int J Hydrogen Energy 2023. https://doi.org/10.1016/j.ijhydene.2023.02.040.
[26] Schiro F, Stoppato A. Experimental investigation of emissions and flame stability for steel and metal fiber cylindrical premixed burners. Combust Sci Technol 2019;191(3):453–71. https://doi.org/10.1080/00102202.2018.1500556.
[27] Boulahlib M, Medaerts F, Boukhalfa M. Experimental study of a domestic boiler using hydrogen methane blend and fuel-rich staged combustion. Int J Hydrogen Energy 2021;46(75):37628–40. https://doi.org/10.1016/j.ijhydene.2021.01.103.
[28] de Vries H, Mokhov AV, Levinsky HB. The impact of natural gas/hydrogen mixtures on the performance of end-use equipment: interchangeability analysis for domestic appliances. Appl Energy 2017;208:1007–19. https://doi.org/10.1016/j.apenergy.2017.09.049.
[29] Aniello A, Poinsot T, Selle L, Schuller T. Hydrogen substitution of natural-gas in premixed burners and implications for blow-off and flashback limits. Int J Hydrogen Energy 2022. https://doi.org/10.1016/j.ijhydene.2022.07.066.
[30] Lewis B, von Elbe G. Stability and structure of burner flames. J Chem Phys 1943;11(2):75–97. https://doi.org/10.1063/1.1723808.
[31] Hertzberg M. Flame stretch extinction in flow gradients, flammability limits under natural convection. vol. 20 (1). In: Symposium (international) on combustion; 1985. p. 1967–74. https://doi.org/10.1016/S0082-0784(85)80696-2.
[32] Zhang W, Wang J, Lin W, Mao R, Xia H, Zhang M, Huang Z. Effect of differential diffusion on turbulent lean premixed hydrogen enriched flames through structure analysis. Int J Hydrogen Energy 2020;45(18):10920–31. https://doi.org/10.1016/j.ijhydene.2020.02.032.
[33] Prasad TG, Jithin E, Varghese RJ, Kumar S, Mohammad A, Velamati RK. Effect of hydrocarbon addition on tip opening of hydrogen-air bunsen flames. Int J Hydrogen Energy 2021;46(7):5763–75. https://doi.org/10.1016/j.ijhydene.2020.10.166.
[34] Law C. Dynamics of stretched flames. vol. 22 (1). In: Symposium (international) on combustion; 1989. p. 1381–402. https://doi.org/10.1016/S0082-0784(89)80149-3.
[35] Altay HM, Kedia KS, Speth RL, Ghoniem AF. Two-dimensional simulations of steady perforated-plate stabilized premixed flames. Combust Theor Model 2010;14(1):125–54. https://doi.org/10.1080/13647831003660859.
[36] Kedia KS, Ghoniem AF. Mechanisms of stabilization and blowoff of a premixed flame downstream of a heat-conducting perforated plate. Combust Flame 2012;159(3):1055–69. https://doi.org/10.1016/j.combustflame.2011.10.014.
[37] Berger S, Duchaine F, Gicquel LYM. Bluff-body thermal property and initial state effects on a laminar premixed flame anchoring pattern. Flow Turbul Combust 2018;100. https://doi.org/10.1007/s10494-017-9841-y.
[38] Vance F, Shoshin Y, van Oijen J, de Goey L. Effect of Lewis number on premixed laminar lean-limit flames stabilized on a bluff body. Proc Combust Inst 2019;37(2):1663–72. https://doi.org/10.1016/j.proci.2018.07.072.
[39] Vu TM, Cha MS, Lee BJ, Chung SH. Tip opening of premixed bunsen flames: extinction with negative stretch and local Karlovitz number. Combust Flame 2015;162(4):1614–21. https://doi.org/10.1016/j.combustflame.2014.11.022.
[40] Lapenna PE, Berger L, Attili A, Lamioni R, Fogla N, Pitsch H, Creta F. Data-driven subfilter modelling of thermo-diffusively unstable hydrogen–air premixed flames.

Combust Theor Model 2021;25(6):1064–85. https://doi.org/10.1080/13647830.2021.1925350.
[41] Chung S, Law C. An integral analysis of the structure and propagation of stretched premixed flames. Combust Flame 1988;72(3):325–36. https://doi.org/10.1016/0010-2180(88)90131-9.
[42] Altay H, Park S, Wu D, Wee D, Annaswamy A, Ghoniem A. Modeling the dynamic response of a laminar perforated-plate stabilized flame. Proc Combust Inst 2009;32(1):1359–66. https://doi.org/10.1016/j.proci.2008.06.099.
[43] Kurdyumov V, Fernández-Tarrazo E, Truffaut J-M, Quinard J, Wangher A, Searby G. Experimental and numerical study of premixed flame flashback. Proc Combust Inst 2007;31(1):1275–82. https://doi.org/10.1016/j.proci.2006.07.100.
[44] Kıymaz TB, Böncü E, Güleryüz D, Karaca M, Yılmaz B, Allouis C, Gökalp İskender. Numerical investigations on flashback dynamics of premixed methane-hydrogen-air laminar flames. Int J Hydrogen Energy 2022;47(59):25022–33. https://doi.org/10.1016/j.ijhydene.2022.05.230.
[45] Vance F, de Goey L, van Oijen J. Development of a flashback correlation for burner-stabilized hydrogen-air premixed flames. Combust Flame 2022:112045. https://doi.org/10.1016/j.combustflame.2022.112045.
[46] Pers H, Aniello A, Morisseau F, Schuller T. Autoignition-induced flashback in hydrogen-enriched laminar premixed burners. Int J Hydrogen Energy 2023;48(27):10235–49. https://doi.org/10.1016/j.ijhydene.2022.12.041.
[47] Goodwin DG, Moffat HK, Schoegl I, Speth RL, Weber BW. Cantera: an object-oriented software toolkit for chemical kinetics, thermodynamics, and transport processes. 2022. https://www.cantera.org, version 2.6.0.
[48] Geuzaine C, Remacle J-F. Gmsh a 3-D finite element mesh generator with built-in pre-and post-processing facilities. Int J Numer Methods Eng 2009;79(11):1309–31.
[49] Poinsot T, Veynante D. Theoretical and numerical combustion. RT Edwards, Inc.; 2005.
[50] Ansys Inc. Ansys Fluent 22.1 User's guide. 2022.
[51] Stewart WE. Multicomponent mass transfer. AIChE J 1995;41(1):202–3. https://doi.org/10.1002/aic.690410124.
[52] Merk HJ. The macroscopic equations for simultaneous heat and mass transfer in isotropic, continuous and closed systems. Applied Scientific Research, Section A 1959;8(1):73–99. https://doi.org/10.1007/BF00411741.
[53] Bilger R, Stårner S, Kee R. On reduced mechanisms for methane-air combustion in non-premixed flames. Combust Flame 1990;80(2):135–49. https://doi.org/10.1016/0010-2180(90)90122-8.
[54] Aminian J, Galletti C, Shahhosseini S, Tognotti L. Key modeling issues in prediction of minor species in diluted-preheated combustion conditions. Appl Therm Eng 2011;31(16):3287–300. https://doi.org/10.1016/j.applthermaleng.2011.06.007.
[55] Lamioni R, Bronzoni C, Folli M, Tognotti L, Galletti C. Effect of slit pattern on the structure of premixed flames issuing from perforated burners in domestic condensing boilers. Combust Theor Model 2022. https://doi.org/10.1080/13647830.2022.2157753.
[56] Kuo K. Principles of combustion. A Wiley-interscience publications; 1986. Wiley.
[57] Modest M.F. Chapter 17 - the method of Discrete Ordinates (s_n-approximation). In: Modest M.F., editor. Radiative heat transfer. (3rd ed.), Edition Boston: Academic Press; 2013. p. 541–584. https://doi.org/10.1016/B978-0-12-386944-9.50017-0.
[58] Zuo W, E. J, Lin R, Jin Y, Han D. Numerical investigations on different configurations of a four-channel meso-scale planar combustor fueled by hydrogen/air mixture. Energy Convers Manag 2018;160:1–13. https://doi.org/10.1016/j.enconman.2018.01.033.
[59] Cai T, Sun Y, Zhao D. Enhancing heat transfer performance analyses of a hydrogen-fueled meso-combustor with staggered bluff-bodies. Fuel Process Technol 2021;218:106867. https://doi.org/10.1016/j.fuproc.2021.106867.
[60] Tan Y, E. J, Chen J, Liao G, Zhang F, Li J. Investigation on combustion characteristics and thermal performance of a three rearward-step structure micro combustor fueled by premixed hydrogen/air. Renew Energy 2022;186:486–504. https://doi.org/10.1016/j.renene.2022.01.019.